



ANL-ART-240
ANL-METL-35

Thermal Hydraulic Experimental Test Article – Fiscal Year 2021 Final Report

Nuclear Sciences and Engineering Division

About Argonne National Laboratory

Argonne is a U.S. Department of Energy laboratory managed by UChicago Argonne, LLC under contract DE-AC02-06CH11357. The Laboratory's main facility is outside Chicago, at 9700 South Cass Avenue, Argonne, Illinois 60439. For information about Argonne and its pioneering science and technology programs, see www.anl.gov.

DOCUMENT AVAILABILITY

Online Access: U.S. Department of Energy (DOE) reports produced after 1991 and a growing number of pre-1991 documents are available free at OSTI.GOV (<http://www.osti.gov/>), a service of the US Dept. of Energy's Office of Scientific and Technical Information.

Reports not in digital format may be purchased by the public from the National Technical Information Service (NTIS):

U.S. Department of Commerce
National Technical Information
Service 5301 Shawnee Rd
Alexandria, VA 22312
www.ntis.gov
Phone: (800) 553-NTIS (6847) or (703) 605-6000
Fax: (703) 605-6900
Email: **orders@ntis.gov**

Reports not in digital format are available to DOE and DOE contractors from the Office of Scientific and Technical Information (OSTI):

U.S. Department of Energy
Office of Scientific and Technical Information
P.O. Box 62
Oak Ridge, TN 37831-0062
www.osti.gov
Phone: (865) 576-8401
Fax: (865) 576-5728
Email: **reports@osti.gov**

Disclaimer

This report was prepared as an account of work sponsored by an agency of the United States Government. Neither the United States Government nor any agency thereof, nor UChicago Argonne, LLC, nor any of their employees or officers, makes any warranty, express or implied, or assumes any legal liability or responsibility for the accuracy, completeness, or usefulness of any information, apparatus, product, or process disclosed, or represents that its use would not infringe privately owned rights. Reference herein to any specific commercial product, process, or service by trade name, trademark, manufacturer, or otherwise, does not necessarily constitute or imply its endorsement, recommendation, or favoring by the United States Government or any agency thereof. The views and opinions of document authors expressed herein do not necessarily state or reflect those of the United States Government or any agency thereof, Argonne National Laboratory, or UChicago Argonne, LLC.

Thermal Hydraulic Experimental Test Article – Fiscal Year 2021 Final Report

M. Weathered, D. Kultgen, E. Kent, J. Rein, C. Grandy

Nuclear Sciences and Engineering Division
Argonne National Laboratory

September 2021

TABLE OF CONTENTS

1. Executive Summary	1
2. Introduction	3
2.1. System Overview and Systems Code Application.....	4
3. Primary System Component Summary	6
3.1. Transport to METL Facility.....	6
3.2. Secondary Dip Tube Installation	8
3.1. Pump	12
3.2. Primary System Assembly	18
3.3. Instrumentation	21
3.4. Submersible Flowmeter	25
3.5. Installation of Primary Assembly	31
3.6. Data Acquisition and Control Software.....	33
3.7. METL 28” Flange Fastener Improvement.....	34
4. Secondary System	35
4.1. Secondary Flowmeter	35
4.2. Secondary Pump	37
4.3. Intermediate Heat Exchanger.....	37
5. THETA Model Development.....	39
6. Conclusions and Path Forward.....	39
7. Acknowledgements	39
8. References	41

LIST OF FIGURES

Figure 1: THETA primary system	2
Figure 2: Isometric drawing of THETA primary vessel and secondary system left. Location of THETA in METL facility highlighted with red square, right.....	2
Figure 3: THETA installed in METL test vessel #4.....	3
Figure 4: P&ID schematic of THETA	4
Figure 5: THETA pool and core geometry. Core nominal diameter: 0.2 [m] (8”), core heated length: 0.3 [m] (12”)	5
Figure 6: Schematic of SAS4A/SASSYS-1 showing locations of various compressible volumes (CV#) and segments (S#)	6
Figure 7: THETA assembly immediately following removal from 260 gallon polycarbonate vessel used for deionized water testing in Argonne building 206	7
Figure 8: THETA primary flange and inner vessel being picked up from building 206 loading dock.....	7
Figure 9: THETA primary flange and inner vessel being placed on trailer for transport to METL facility	8
Figure 10: Electrical enclosures, pump motor, thermocouples, and sensors prepared for riggers to transport from building 206 water testing facility to building 308 hibay for installation at METL.....	8
Figure 11: THETA being disassembled in building 308 for final modifications and sanitization before reassembly	9
Figure 12: Welding secondary system dip tube connection. Argon purge to purify full penetration weld provided by plastic tube, left. Final welded dip tube connection with 3/4” Swagelok connection for attachment of 3/4” stainless steel dip tube.....	10
Figure 13: 3/4” stainless steel dip tube	10
Figure 14: Final welded secondary system transfer valve on top of the primary system flange. This facilitates transfer of METL sodium from THETA primary system into secondary system with the use of a dip tube, eliminating the need to use a second METL vessel or an auxiliary supply of sodium that would require additional sodium purification infrastructure.	11
Figure 15: Picture of inner vessel hot pool before installation of immersion heater	12
Figure 16: 3D printed THETA 4.5” diameter primary impeller during final conventional machining to bring purposely undersized bore to spec and flatten out all surfaces to ensure balanced operation. This is during machining; the final passes of the mill were finer to produce a smoother finish.	13
Figure 17: Photo showing the vibration sensor installed on the primary pump motor, left, as well as water escaping the top of the column pipe, right.....	14
Figure 18: Water began escaping column pipe, Figure 17, at a speed of 1,150 RPM (flowrate of 11.4 GPM). At 1,100 RPM (11 GPM) there was not water escaping.	14
Figure 19: Column pipe expansion piece shown with 1/8” thermocouple probe mount location highlighted. A thermocouple is installed at this location to determine maximum	

pump performance, before sodium begins to flow out of the top of the column pipe due to high pump case pressure	15
Figure 20: Photo of the 1/8” thermocouple probe mounted to the top of the column pipe to facilitate determination of maximum pump speed before sodium is pushed to the top of the column.	15
Figure 21: Pump motor vibration as a function of motor speed. Pump operating in water at room temperature. Resonant frequencies seen at accelerometer peaks at 1050 RPM and 1600 RPM	16
Figure 22: Pump components in ultrasonic bath for final cleaning	17
Figure 23: Pump debris well after water testing campaign. No graphite debris was evident below the debris well. A complete description of debris well can be found in [1], [2]	17
Figure 24: Dial indicator on bottom of pump shaft where impeller is mounted showed acceptable shaft runout of ± 0.005 ” before final assembly.....	18
Figure 25: Inner vessel following final cleaning	19
Figure 26: THETA primary piping	20
Figure 27: Photo showing various features of the THETA cold pool. Note that the 13 junctions on one of the QTY (3) thermocouple rakes have been highlighted with yellow circles.	21
Figure 28: THETA instrumentation port locations.....	23
Figure 29: Instrumentation adapter 1/2” Swagelok VCR fitting (right side) to Conax Compression Seal fitting with graphite sealant (left side) to accommodate QTY (4) 1/8” diameter sensors	23
Figure 30: LEFT: intermediate heat exchanger outlet showing 1/8” multijunction thermocouple probe with junctions at the center of each of the 6 outlets. 0.008” thick 316 stainless steel sheet metal was used to fix the position of the probe. QTY (6) thermocouple junction locations were highlighted with yellow circles for clarity. RIGHT: Temperature is read on the outer surface of the inner vessel with the use of a 1/8” multijunction thermocouple probe. QTY (16) thermocouple junction locations were highlighted with yellow circles for clarity.	24
Figure 31: Electromagnetic flowmeter installed in THETA primary piping. All 316 stainless steel Grayloc assemblies with Inconel uncoated seal rings are used.	25
Figure 32: Custom built single point continuity level detector. All stainless steel and alumina construction. BNC connector for sensor reading	25
Figure 33: Photo showing the Instrument Under Test (IUT) and the Reference (REF) flowmeter installed in the University of Wisconsin-Madison liquid sodium calibration loop. The loop possesses a moving magnet pump that is controlled by a variable frequency drive	26
Figure 34: Sealing off signal wire feedthrough on THETA primary flowmeter.	26
Figure 35: Vacuum/helium backfill port TIG welded shut.....	27
Figure 36: Setup to facilitate pulling vacuum and backfilling flowmeter cavity with helium.	27
Figure 37: Helium leak detector showing hard vacuum of <1 milli Torr pulled on assembly and a helium presence of $<10^{-8}$ atm-cc/sec in the internal cavity of the flowmeter	

where signal wires, thermocouple and magnets reside. Helium gas was passed across all surfaces of the flowmeter.....	28
Figure 38: Photo of completed THETA submersible electromagnetic flowmeter with 15” ruler for reference. Note the 1/8” MI cables transmitting temperature and sensor data have been spooled up for easy transport.....	28
Figure 39: Velocity in the x direction, U_x , with black streamlines showing magnetic flux density through the cross section of the flow tube and permanent magnets. T_m and T_s at 400 °C, $Q= 83.3$ LPM (22 GPM) [4]	29
Figure 40: Experimental and FEA induced voltage as a function of sodium flowrate at 400 and 220°C. FEA results deviate <3.2% from experimental trendline. Error bars have been provided for EMFM voltage and reference flow rate, representing type A and B uncertainty in the 90 measurements taken for each flow rate and temperature [4]	30
Figure 41: Installation of THETA into METL with building 308 overhead crane.....	31
Figure 42: Installation of THETA into METL with building 308 overhead crane.....	32
Figure 43: THETA with flange heaters, insulation, pump motor, and all thermocouples and instrumentation installed.....	32
Figure 44: THETA electrical control cabinets installed on METL mezzanine, north wall.....	33
Figure 45: Labview based graphical user interface, THETA data acquisition and control software.....	34
Figure 46: 1-1/2” 304SS flange bolt with galling.....	34
Figure 47: Significant galling was seen when pairing 304 stainless steel nuts with 304 stainless steel bolts to mount the THETA flange to the METL vessel, even with the use of nuclear grade high temperature anti-seize. 1-1/2”-12 heavy hex nuts in Inconel 718, SB-637 with silver coating were acquired to mate with the stainless steel flange bolts	35
Figure 48: Secondary flowmeter isometric view (left), view with grating removed to reveal important constituent components (right).....	36
Figure 49: Secondary flowmeter surfaces with convection coefficient set to 1 W/m ² K shown in blue, all other surfaces adiabatic (left). Surface temperature profile with flow pipe temperature set to 670 °C (right).	36
Figure 50: COMSOL Multiphysics study, cross section looking down flow pipe at the center of the magnet/yoke assembly showing the electric potential and magnetic flux density at a sodium flowrate of 5 GPM	37
Figure 51: THETA secondary pump and pump curves	37
Figure 52: THETA IHX side view.....	38
Figure 53: IHX view showing the downcomer/upcomers and baffles	38
Figure 54: Cross section showing the two thermal expansion bellows and the downcomer vacuum snorkel	39

LIST OF TABLES

Table 1: THETA instrumentation and measurement. Port positions provided in Figure 28	22
Table 2: Electromagnetic Flowmeter Uncertainty Budget [4].....	30

1. Executive Summary

The Thermal Hydraulic Experimental Test Article (THETA) is a facility that will be used to develop sodium components and instrumentation as well as acquire experimental data for validation of reactor thermal hydraulic and safety analysis codes. The facility will simulate nominal conditions as well as protected/unprotected loss of flow accidents in a sodium-cooled fast reactor (SFR). High fidelity distributed temperature profiles of the developed flow field will be acquired with Rayleigh backscatter based optical fiber temperature sensors. The facility is being designed in partnership with systems code experts to tailor the experiment to ensure the most relevant and highest quality data for code validation.

THETA is comprised of a traditional primary and secondary system. The primary system is submerged in the pool of sodium and consists of a pump, electrically heated core, intermediate heat exchanger, and connected piping and thermal barriers (redan). The secondary system, located outside of the sodium pool, consists of a pump, sodium to air heat exchanger, and connected piping and valves.

Figure 1 illustrates the main components of the primary system. THETA has been installed in the Mechanisms Engineering Test Loop (METL) with the primary system in the 28 inch Test Vessel #4, Figure 2 and Figure 3. Since the FY20 THETA status report, [1], further water shakedown testing was performed, some final welding modifications were performed, all system components were sanitized, dry assembled, and commissioned. The THETA submersible electromagnetic flowmeter was welded closed to hermetically seal internal components from sodium followed by a helium leak check for the final time.

Following installation of THETA into vessel #4, all data acquisition and control systems were brought online and commissioned at room temperature in the argon gas space of the empty vessel. The vessel zone 1 heaters were reinstalled and the flange was then insulated. The vessel 4 heaters were brought to a temperature of 100 °C and the THETA pump was jogged at 600 RPM to ensure it was functioning correctly.

The secondary, AC Conduction based electromagnetic pump from CMI Novacast (product number CA-15) was ordered and will be delivered in late calendar year 2021. The custom designed permanent magnet based secondary flowmeter was designed, a drawing package and manufacturing specification created and quote requested from a machine shop. The intermediate heat exchanger design was completed and a drawing package is currently in progress.

During the middle of calendar year 2021 the Building 308 sodium scrubber system was shut down in order to replaced some corroded piping and facilitate improvements on the system, thus requiring the sodium in METL to remain frozen. This has imposed a delay in filling vessel 4 with sodium to begin THETA testing. Sodium testing is expected to begin in early fiscal year 2022 as all THETA primary systems are operational.

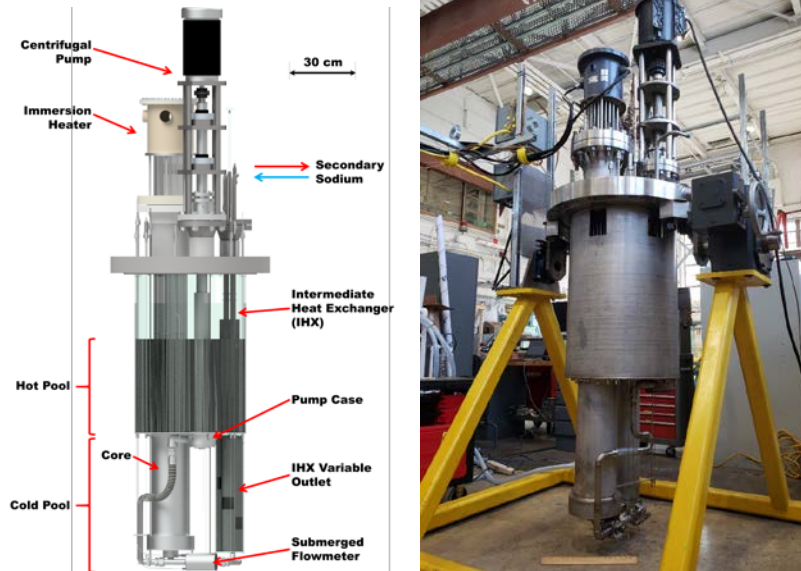


Figure 1: THETA primary system

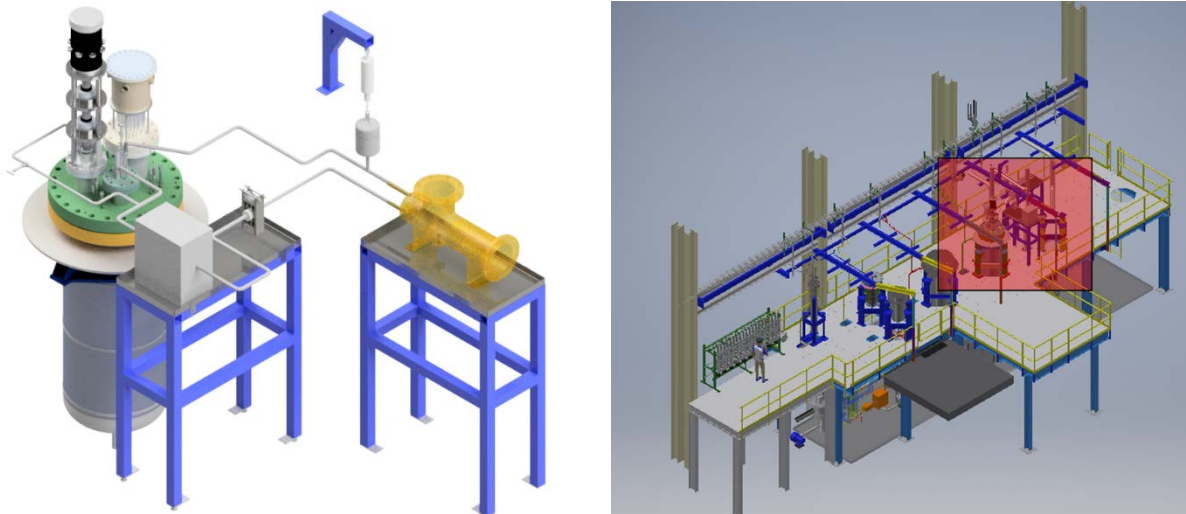


Figure 2: Isometric drawing of THETA primary vessel and secondary system left. Location of THETA in METL facility highlighted with red square, right.



Figure 3: THETA installed in METL test vessel #4

2. Introduction

The Thermal Hydraulic Experimental Test Article (THETA) is a METL vessel experiment designed for testing and validating sodium fast reactor components and phenomena. THETA has been scaled using a non-dimensional Richardson number approach to represent temperature distributions during nominal and loss of flow conditions in a sodium fast reactor (SFR), this analysis was detailed in the THETA FY19 report [2]. The facility is being constructed with versatility in mind, allowing for the installation of various immersion heaters, heat pipes, and heat exchangers without significant facility modification. THETA is being designed in collaboration

with systems code experts to inform the geometry and sensor placement to acquire the highest value code validation data.

2.1. System Overview and Systems Code Application

THETA possesses all the major thermal hydraulic components of a pool type sodium cooled reactor. Figure 4 shows the piping and instrumentation diagram (P&ID) for the primary and secondary sodium circuit. A cross section of the primary vessel shows the pool and core geometry, Figure 5. As can be seen, a 28" METL test vessel is used for the primary sodium "reactor" vessel. An isometric model of the primary/secondary vessels, inter-vessel piping, and air-to-sodium heat exchanger (AHX) can be found in Figure 2.

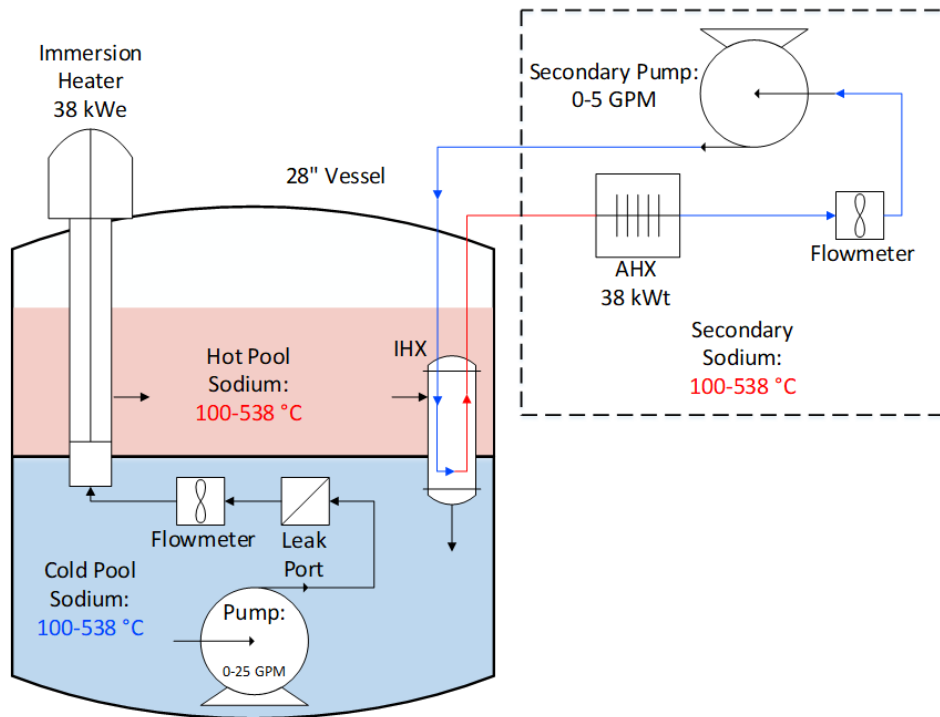


Figure 4: P&ID schematic of THETA

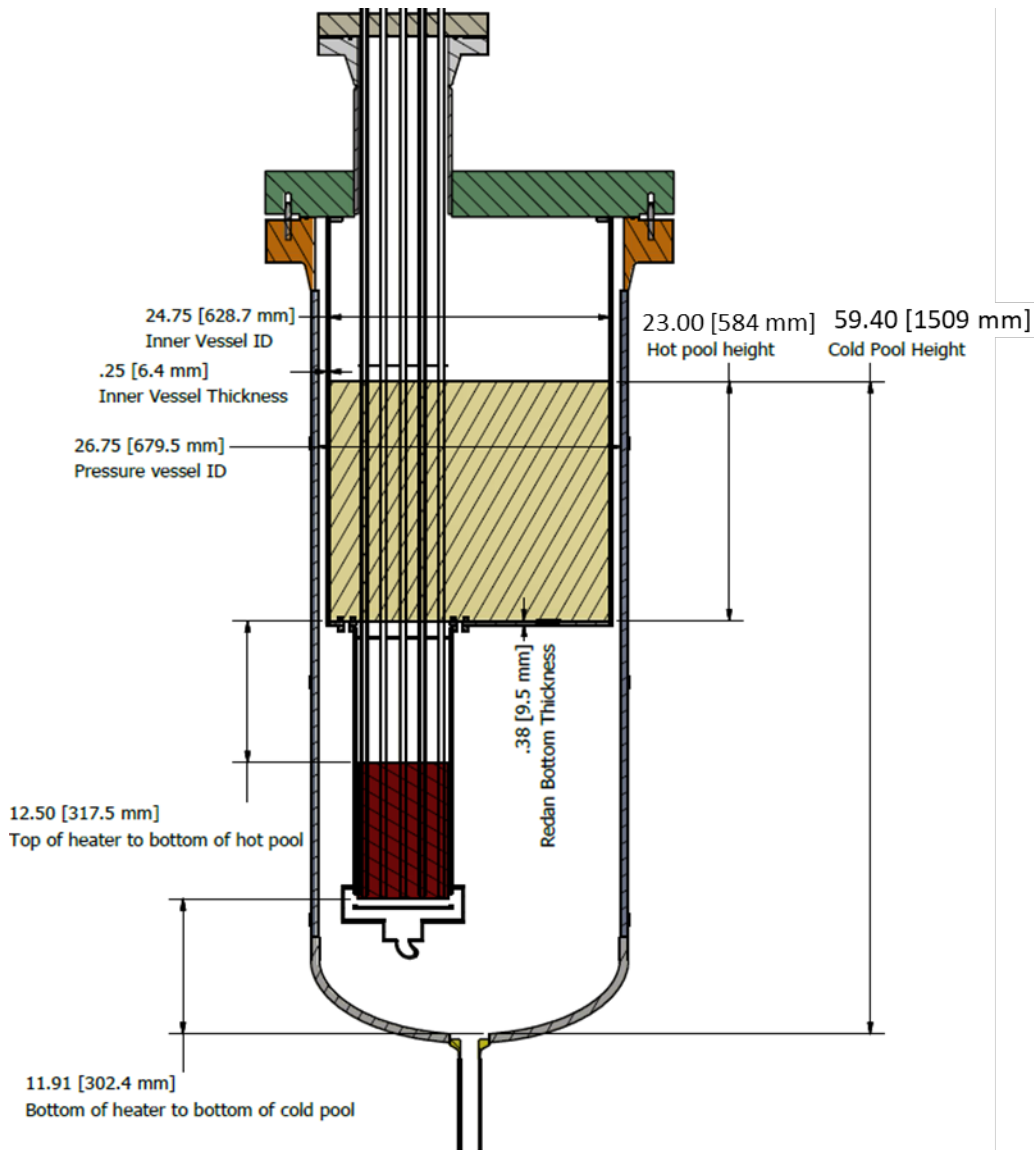


Figure 5: THETA pool and core geometry. Core nominal diameter: 0.2 [m] (8”), core heated length: 0.3 [m] (12”)

Argonne National Laboratory’s SAS4A/SASSYS-1 computer code is used for thermal hydraulic and safety analysis of power and flow transients in liquid metal cooled reactors. Figure 6 gives a graphic displaying the segments and compressible volumes used to perform the deterministic analysis of anticipated events such as protected/un-protected loss of flow reactor trips etc. While SAS4A/SASSYS-1 was benchmarked against tests in historic reactors, such as EBR-II [3], a modern liquid metal thermal hydraulic facility is required for further system’s code validation. Please see [2] for an overview of the current systems code modeling efforts as applied to THETA.

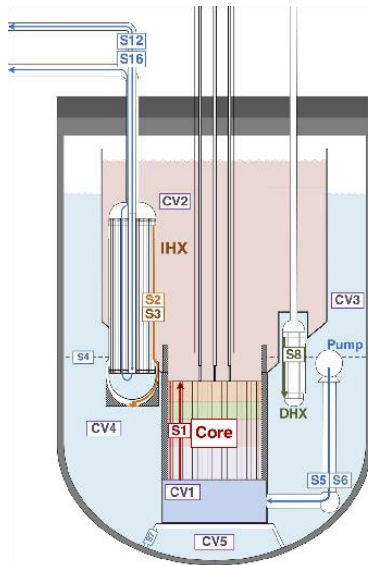


Figure 6: Schematic of SAS4A/SASSYS-1 showing locations of various compressible volumes (CV#) and segments (S#)

3. Primary System Component Summary

The following section presents a summary of all primary system components as of September 2021 - Figure 1 provides a schematic of the primary system for reference. The primary system was tested with deionized water in FY20 and early FY21 at Argonne's Building 206 [1]. The system was then transported to Building 308 where the Mechanisms Engineering Test Loop (METL) is located. The system was disassembled for modifications to improve performance, as informed by the deionized water campaign. The primary system was then sanitized, rinsed and dried for final reassembly. Once reassembled, and all sensors function tested and locations documented, the system was commissioned and installed in the METL 28" test vessel #4.

3.1. Transport to METL Facility

Following the water shakedown/testing campaign, the facility was partially disassembled to facilitate transport from the water testing facility in Argonne building 206, to the METL facility in Argonne Building 308. Figure 7 provides a photo of THETA after removal from polycarbonate vessel following water testing. Figure 8 and Figure 9 show images of THETA being transported on the yellow test article A-frame mount with the use of a fork truck and tractor/trailer. All of the electrical enclosures and auxiliary equipment were disconnected from power and placed on pallets to facilitate their move to the METL facility, Figure 10.



Figure 7: THETA assembly immediately following removal from 260 gallon polycarbonate vessel used for deionized water testing in Argonne building 206



Figure 8: THETA primary flange and inner vessel being picked up from building 206 loading dock



Figure 9: THETA primary flange and inner vessel being placed on trailer for transport to METL facility



Figure 10: Electrical enclosures, pump motor, thermocouples, and sensors prepared for riggers to transport from building 206 water testing facility to building 308 hibay for installation at METL

3.2. Secondary Dip Tube Installation

Once THETA arrived at the METL facility, the test article was disassembled to facilitate final welding modifications as well as a thorough sanitization. Figure 11 shows the inner vessel being removed to expose the underside of the flange to allow for installation of the secondary system dip tube.

Figure 12 shows the mounting fixture for the THETA secondary system dip tube being welded into position. The mount possesses a 3/4" Swagelok compression tube fitting whereby a 3/4" stainless steel dip tube may be fixed, Figure 13. The dip tube sodium is transported through the

THETA flange to the secondary system fill valve, Figure 14. This fill valve is a Swagelok welded bellows valve. All welds above the flange, where sodium-atmosphere leaks could occur, were radiographed in the shop, where possible. Field welds on the secondary system will be radiographed once the secondary system is attached to THETA, before filling with sodium, bringing the secondary system to 100% radiographed welds prior to filling. Helium leak check will also be performed in the field with a mass spectrometer leak detector before charging with sodium as the final non-destructive test of the system. The dip tube can be seen installed in the system in Figure 15.



Figure 11: THETA being disassembled in building 308 for final modifications and sanitization before reassembly



Figure 12: Welding secondary system dip tube connection. Argon purge to purify full penetration weld provided by plastic tube, left. Final welded dip tube connection with 3/4" Swagelok connection for attachment of 3/4" stainless steel dip tube.



Figure 13: 3/4" stainless steel dip tube

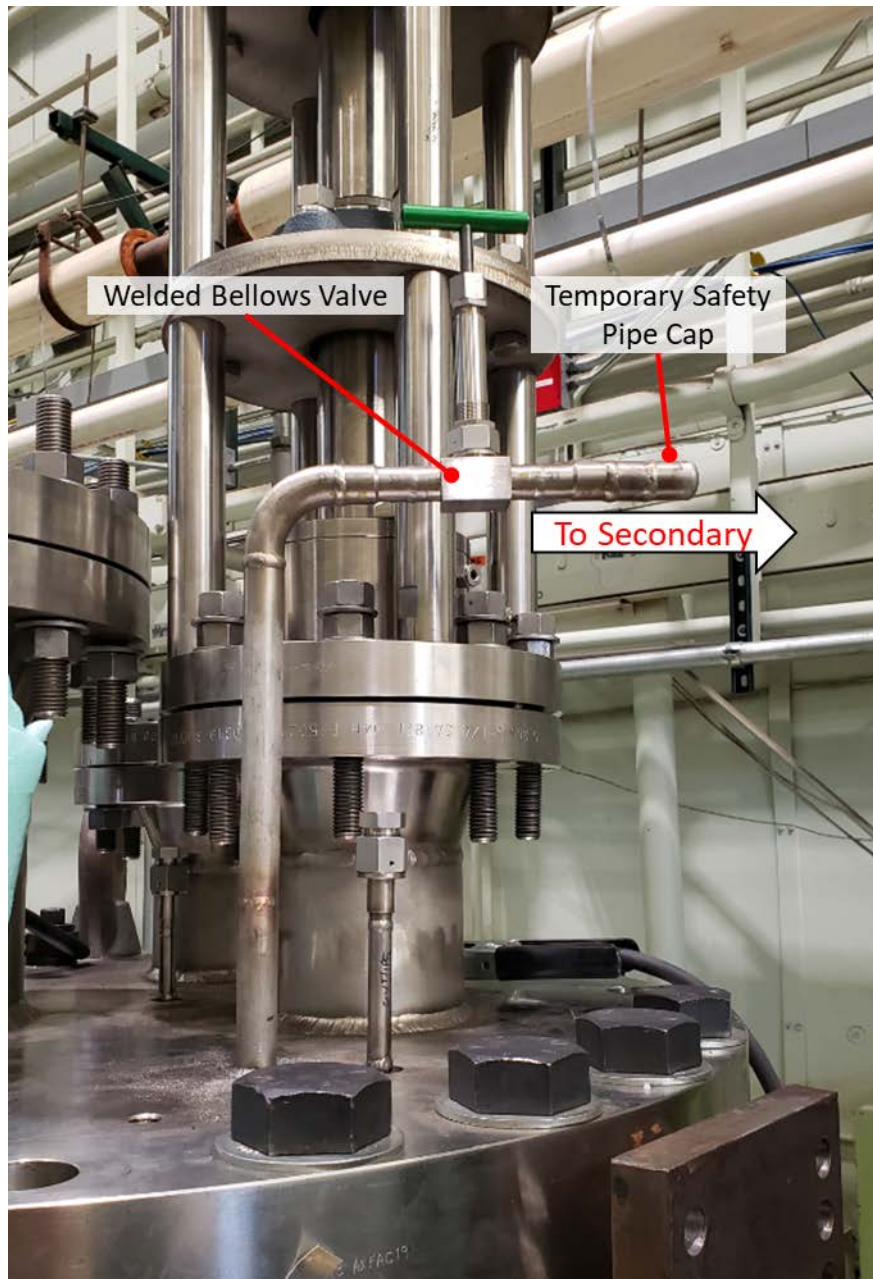


Figure 14: Final welded secondary system transfer valve on top of the primary system flange. This facilitates transfer of METL sodium from THETA primary system into secondary system with the use of a dip tube, eliminating the need to use a second METL vessel or an auxiliary supply of sodium that would require additional sodium purification infrastructure.

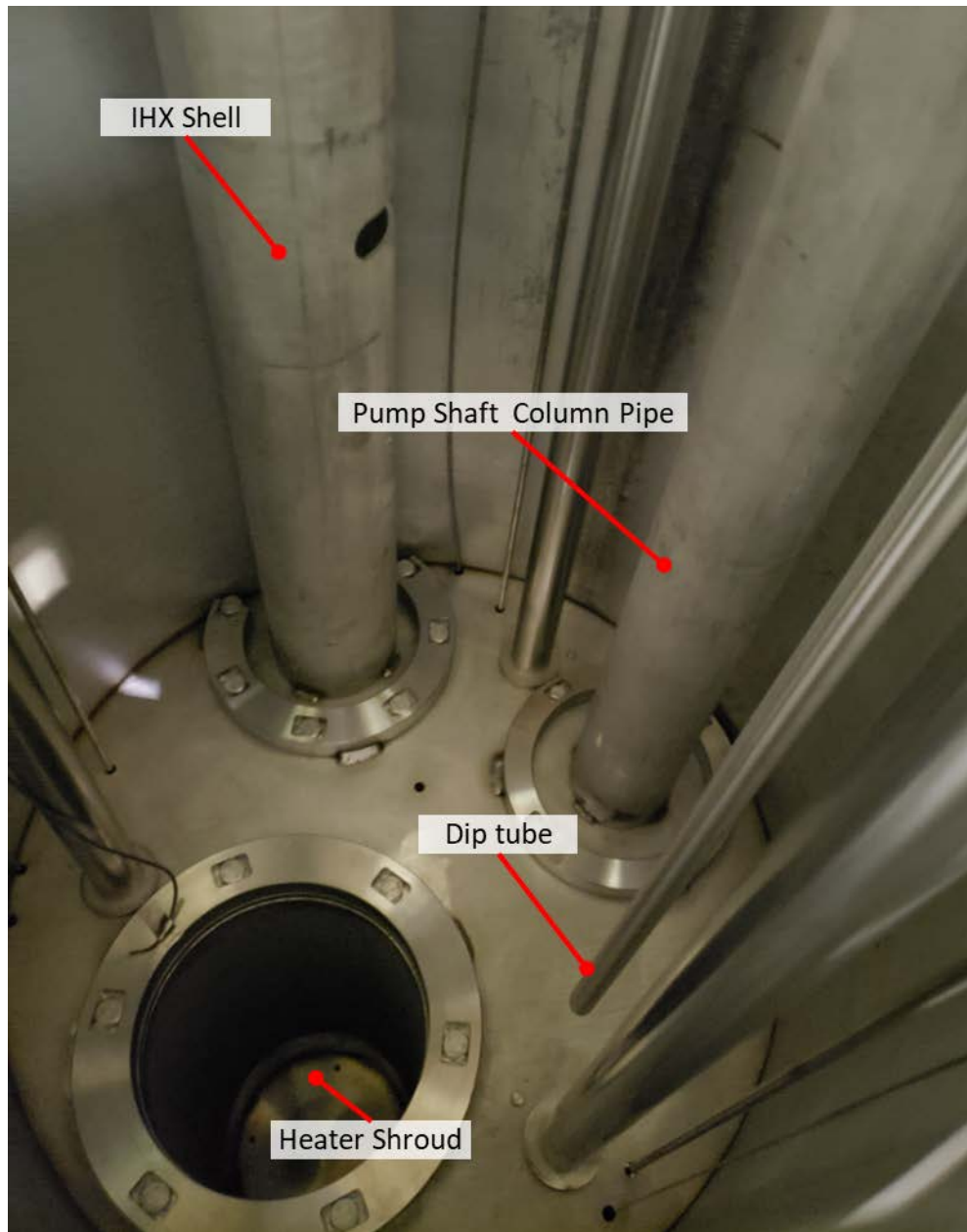


Figure 15: Picture of inner vessel hot pool before installation of immersion heater

3.1.Pump

As mentioned in [1] the THETA primary pump impeller was 3D printed in 316 stainless steel. Final machining was performed on the impeller to expand the undersized bore to the correct clearance to mate with the pump shaft (3D printed tolerances were not sufficiently tight so the bore was purposely undersized to facilitate conventional machining) Figure 16. In addition, all of the surfaces were passed over with the mill to remove the minimum required material to bring all surfaces parallel to a single datum plane. This ensures balanced operation without vibration.



Figure 16: 3D printed THETA 4.5” diameter primary impeller during final conventional machining to bring purposely undersized bore to spec and flatten out all surfaces to ensure balanced operation. This is during machining; the final passes of the mill were finer to produce a smoother finish.

During water testing, water was seen escaping the top of the pump column pipe due to pressure in the pump case building up and leaking through the labyrinth seal, seal described in [1]. Figure 17 shows a photo of the water escaping the top of the column pipe at around 1,150 RPM (water flowrate of 11.4 GPM). Figure 18 shows the pump speed vs flowrate relevant to this testing.

In order to enhance the performance of the pump, the column pipe inner diameter was enlarged from 3.26 to 4.26” and length was extended by 4” at the top with the use of a welded on expansion piece, Figure 19. This effectively provides more volume for the sodium at the top of the column pipe to reside before leaking into the hot pool sodium. As can be seen, there is an 1/8” Swagelok compression fitting at the very top of the expansion piece to mount a thermocouple probe. This allows for determination of maximum pump speed before sodium begins to leak out of the top of the column pipe as a discrete rise in temperature will be seen when the high thermal conductivity sodium touches the thermocouple. Figure 20 provides a photo of this thermocouple as installed.

A vibration sensor (IFM Efector Inc, PN UW0006) was added to the pump motor to determine resonant frequencies of the pump shaft as the speed of the shaft was increased from 0-1800+ RPM in water at room temperature. The vibration sensor location was highlighted in Figure 17 and vibration sensor data provided in Figure 21. As can be seen there is a resonant frequency at 1050 RPM as well as at 1.5x this speed at 1600 RPM. It is best not to operate at these particular speeds

as the shaft vibration could cause premature wear of the graphite seal, rubbing of the labyrinth seal and signal noise in the sensitive optical fiber instrumentation.



Figure 17: Photo showing the vibration sensor installed on the primary pump motor, left, as well as water escaping the top of the column pipe, right.

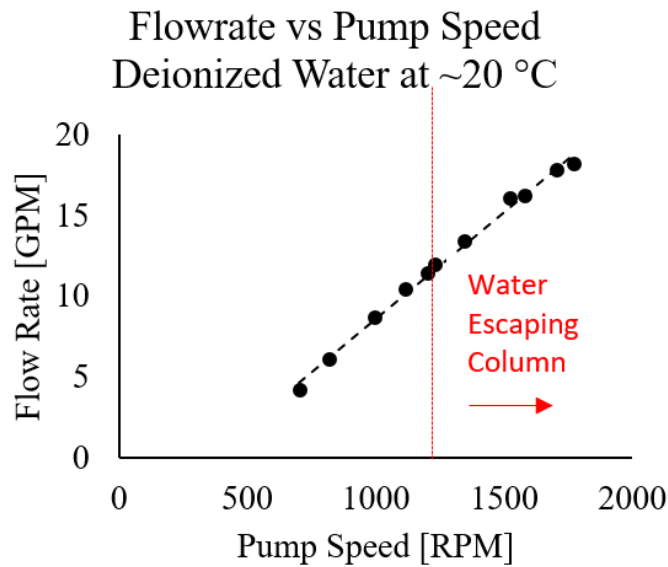


Figure 18: Water began escaping column pipe, Figure 17, at a speed of 1,150 RPM (flowrate of 11.4 GPM). At 1,100 RPM (11 GPM) there was not water escaping.

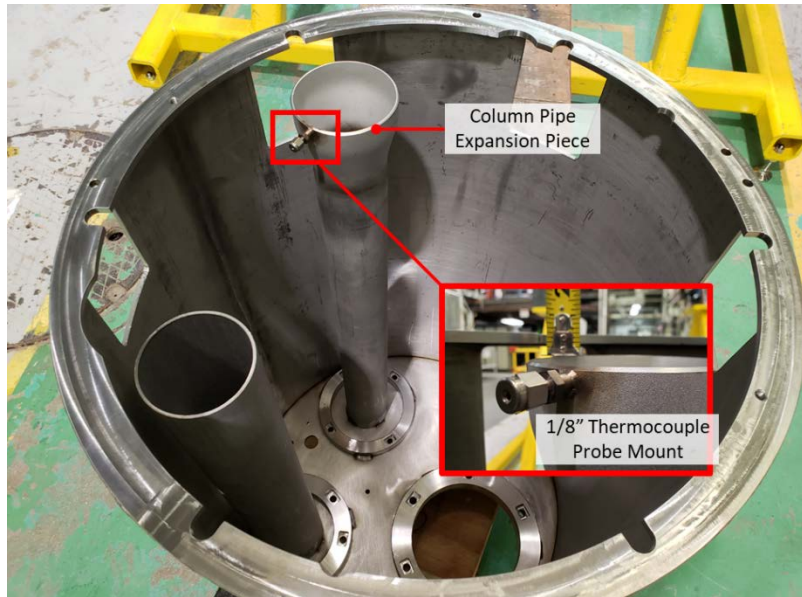


Figure 19: Column pipe expansion piece shown with 1/8" thermocouple probe mount location highlighted. A thermocouple is installed at this location to determine maximum pump performance, before sodium begins to flow out of the top of the column pipe due to high pump case pressure



Figure 20: Photo of the 1/8" thermocouple probe mounted to the top of the column pipe to facilitate determination of maximum pump speed before sodium is pushed to the top of the column.

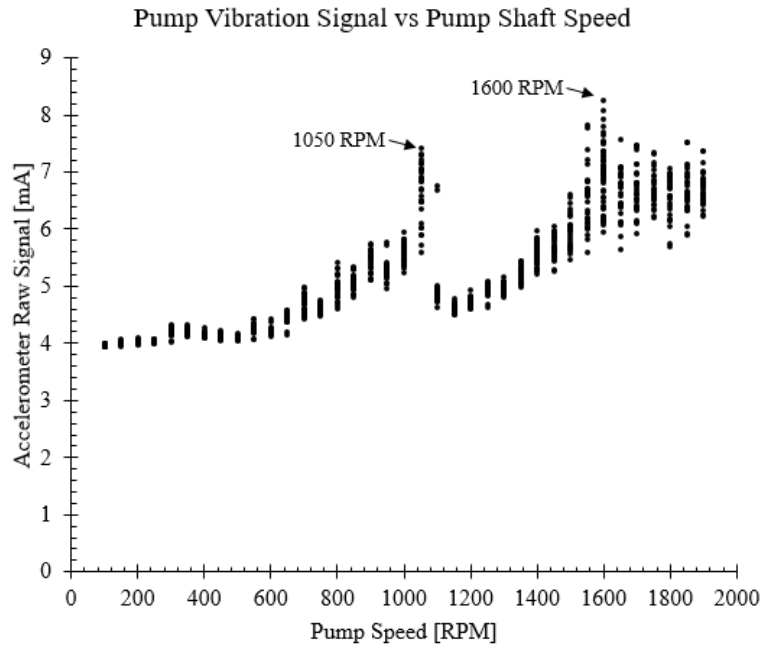


Figure 21: Pump motor vibration as a function of motor speed. Pump operating in water at room temperature. Resonant frequencies seen at accelerometer peaks at 1050 RPM and 1600 RPM

After water testing and transport from Building 206 to Building 308, the pump was disassembled and sanitized with a 1% dilution ratio of Alconox 1125 (a non-halogen based, gentle detergent) and deionized water wash followed by a deionized water rinse, Figure 22. A very small amount of graphite seal debris was seen in the debris well, Figure 23, after the extensive water testing campaign. There was no other evidence of graphite in the system, thus the graphite thrower and debris well are performing as designed, [1], [2].

After cleaning, the pump was reassembled and runout at the bottom of the pump shaft where the pump impeller is mounted was measured with a dial indicator. A reading of ± 0.005 " was measured, this is within acceptable specification, Figure 24.



Figure 22: Pump components in ultrasonic bath for final cleaning

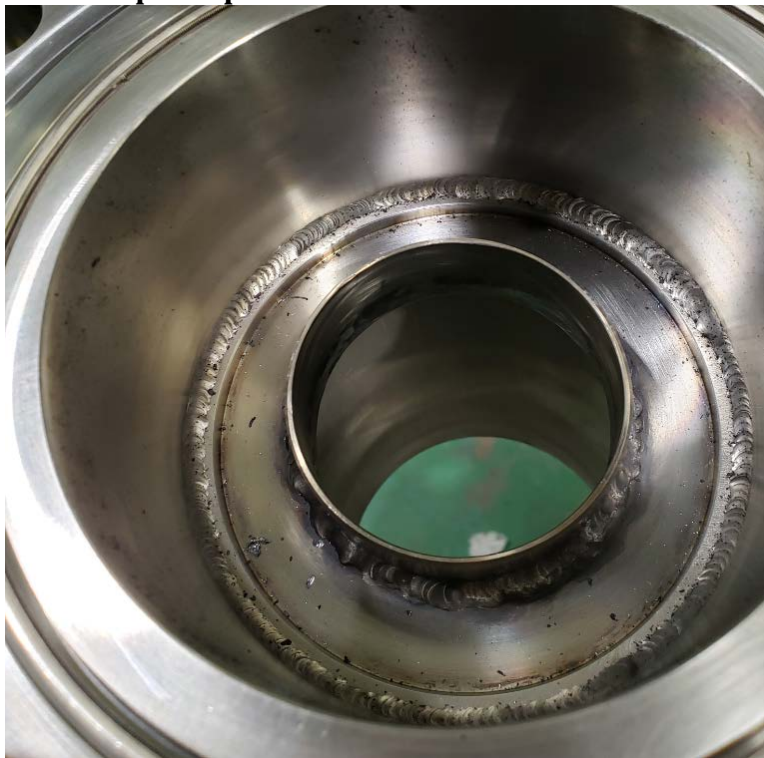


Figure 23: Pump debris well after water testing campaign. No graphite debris was evident below the debris well. A complete description of debris well can be found in [1], [2]



Figure 24: Dial indicator on bottom of pump shaft where impeller is mounted showed acceptable shaft runout of ± 0.005 " before final assembly.

3.2.Primary System Assembly

The primary system components were sanitized with the use of a 1% dilution ratio of Alconox 1125 (a non-halogen based, gentle detergent) and deionized water wash followed by a thorough rinse of deionized water. Figure 25 shows the inside of the inner vessel after cleaning. Figure 26 and Figure 27 shows the cold pool system components and sensors assembled, following cleaning. Components were determined clean when after a lint free laboratory wipe was passed across its surface there was no visible contamination on the wipe.

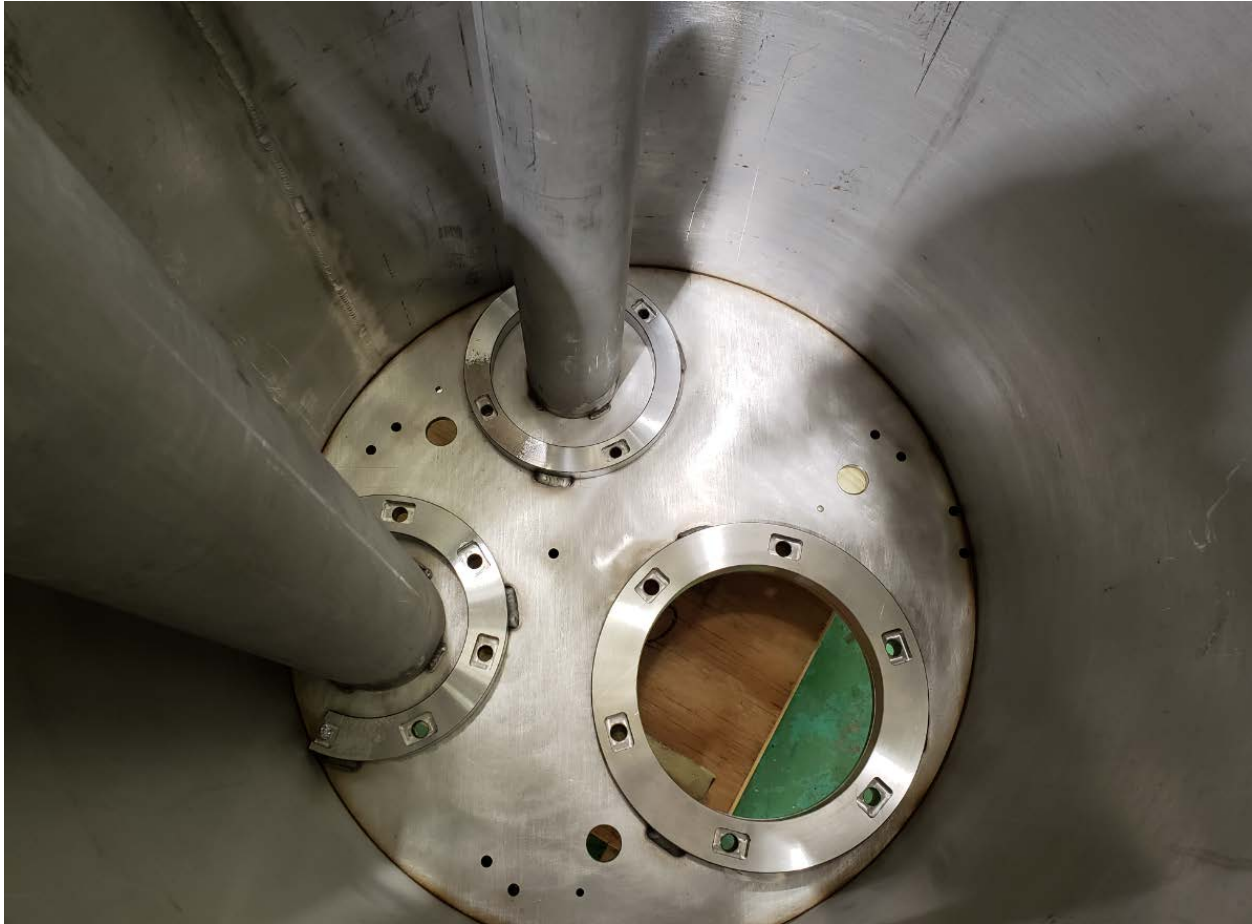


Figure 25: Inner vessel following final cleaning

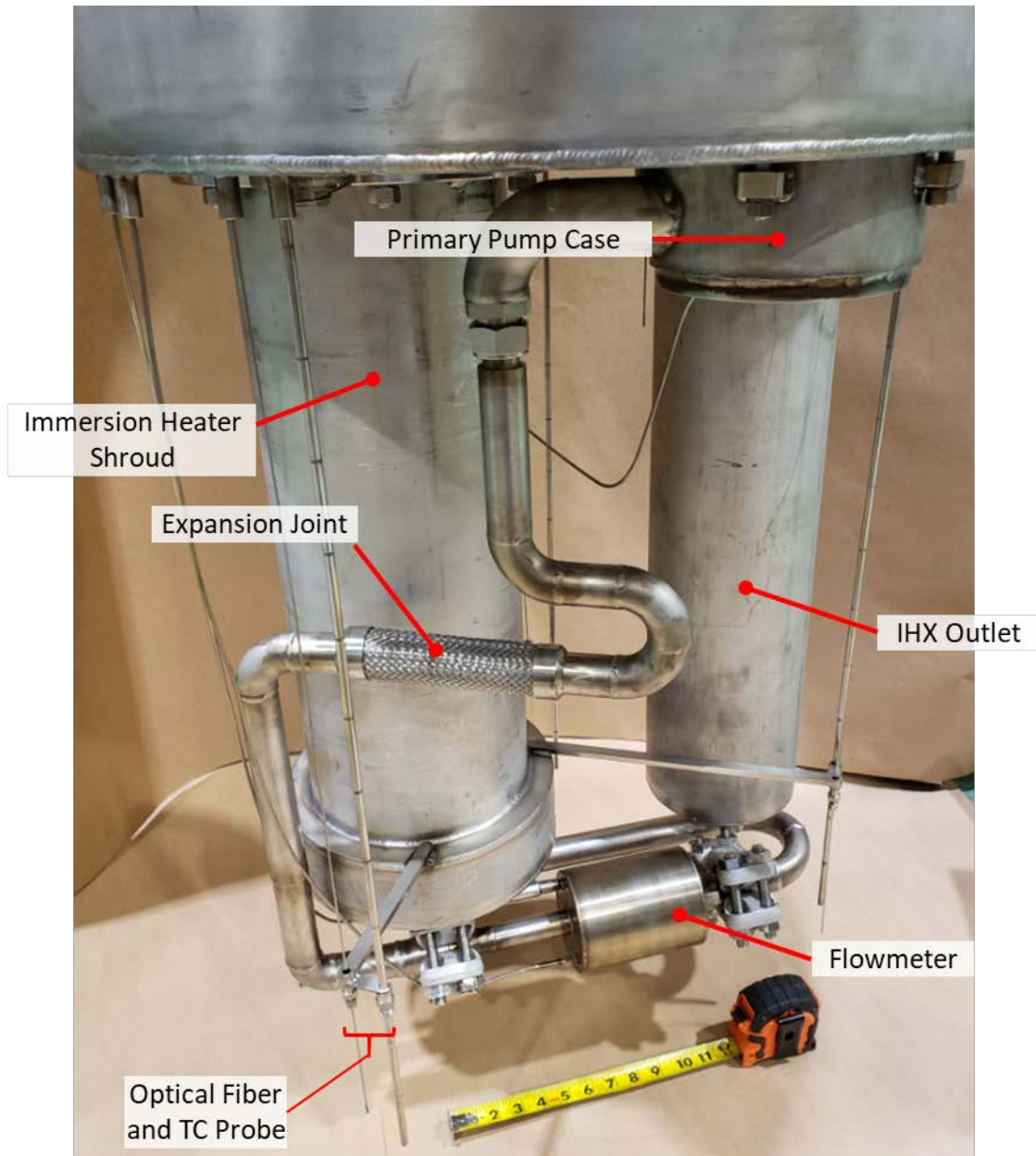


Figure 26: THETA primary piping

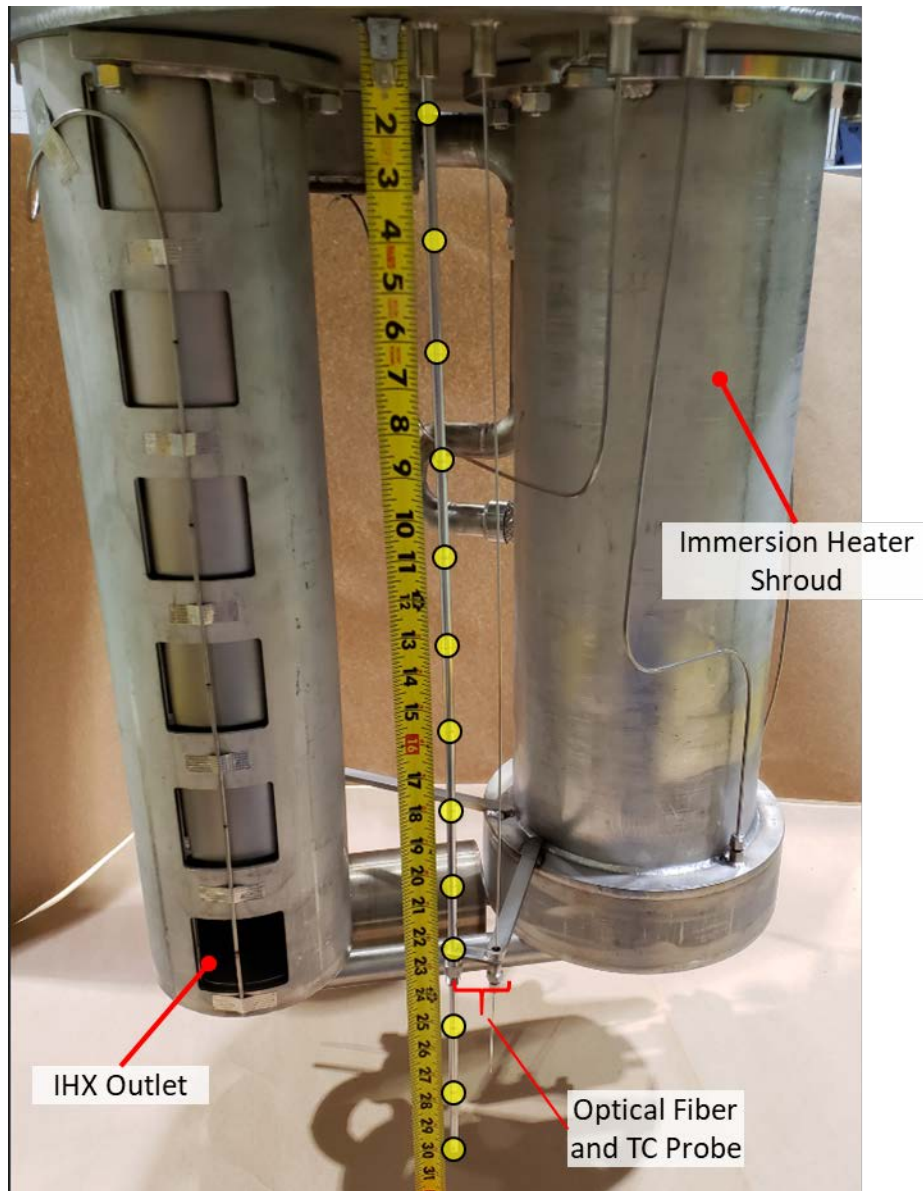


Figure 27: Photo showing various features of the THETA cold pool. Note that the 13 junctions on one of the QTY (3) thermocouple rakes have been highlighted with yellow circles.

3.3. Instrumentation

Table 1 summarizes THETA instrumentation which includes single and multi-point thermocouples, distributed optical fiber temperature sensors, level sensor, and flowmeter voltage measurements. The port locations on the top flange have been labeled in Figure 28. Notice that Ports 1, 5, and 12 have all been expanded four-fold to ports 1a, 1b, 1c, 1d, etc. This was achieved with the use of a custom fabricated adapter that mates a Conax connector with QTY (4) 0.125” feedthroughs with the existing 1/2” Swagelok VCR fitting, Figure 29.

Table 1: THETA instrumentation and measurement. Port positions provided in Figure 28

Port	Instrument	Measurement
1a	Single TC	Pump inlet temperature
1b	Single TC	Core inlet temperature
1c	Blank	-
1d	Blank	-
2	Single TC	Core outlet temperature
3	Fiber	Hot and cold pool distributed axial temperature
4	Rake TC	Hot and cold pool distributed axial temperature
5a	Rake TC	IHX outlet and inner vessel near wall temperature
5b	Single TC	Pump shaft column overflow temperature
5c	Blank	-
5d	Blank	-
6	Rake TC	Hot and cold pool distributed axial temperature
7	Fiber	Hot and cold pool distributed axial temperature
8	Rake TC	Inner vessel near wall temperature in cold pool
9	Rake TC	Hot and cold pool distributed axial temperature
10	Fiber	Hot and cold pool distributed axial temperature
11	Level Sensor	Sodium hot pool at 23” in elevation
12a	MI Cable	Flowmeter voltage
12b	Single TC	Flowmeter temperature
12c	Blank	-
12d	Blank	-
13	Fiber	Hot and cold pool distributed axial temperature
14	Fiber	IHX distributed axial temperature
15	Rake TC	IHX distributed axial temperature
16-20	Single TCs	Core temperature 3” above bottom of elements

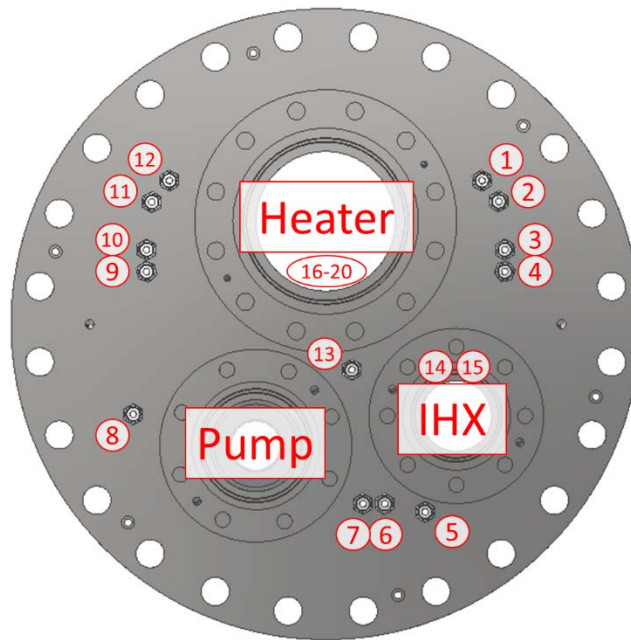


Figure 28: THETA instrumentation port locations



Figure 29: Instrumentation adapter 1/2" Swagelok VCR fitting (right side) to Conax Compression Seal fitting with graphite sealant (left side) to accommodate QTY (4) 1/8" diameter sensors

The IHX outlet temperature thermocouple rake that acquires IHX outlet temperatures at each of the 6 elevations was mounted with the use of a capacitive discharge spot welder. As can be seen in Figure 30, 0.008" thick 316 stainless steel sheet metal was used to fix the thermocouple probe to the IHX outlet assembly by spot welding the sheet metal tight on either side of the probe.

The same spot welding process was used to mount the thermocouple rake that acquires near wall temperatures of the inner vessel in the cold pool, Figure 30.

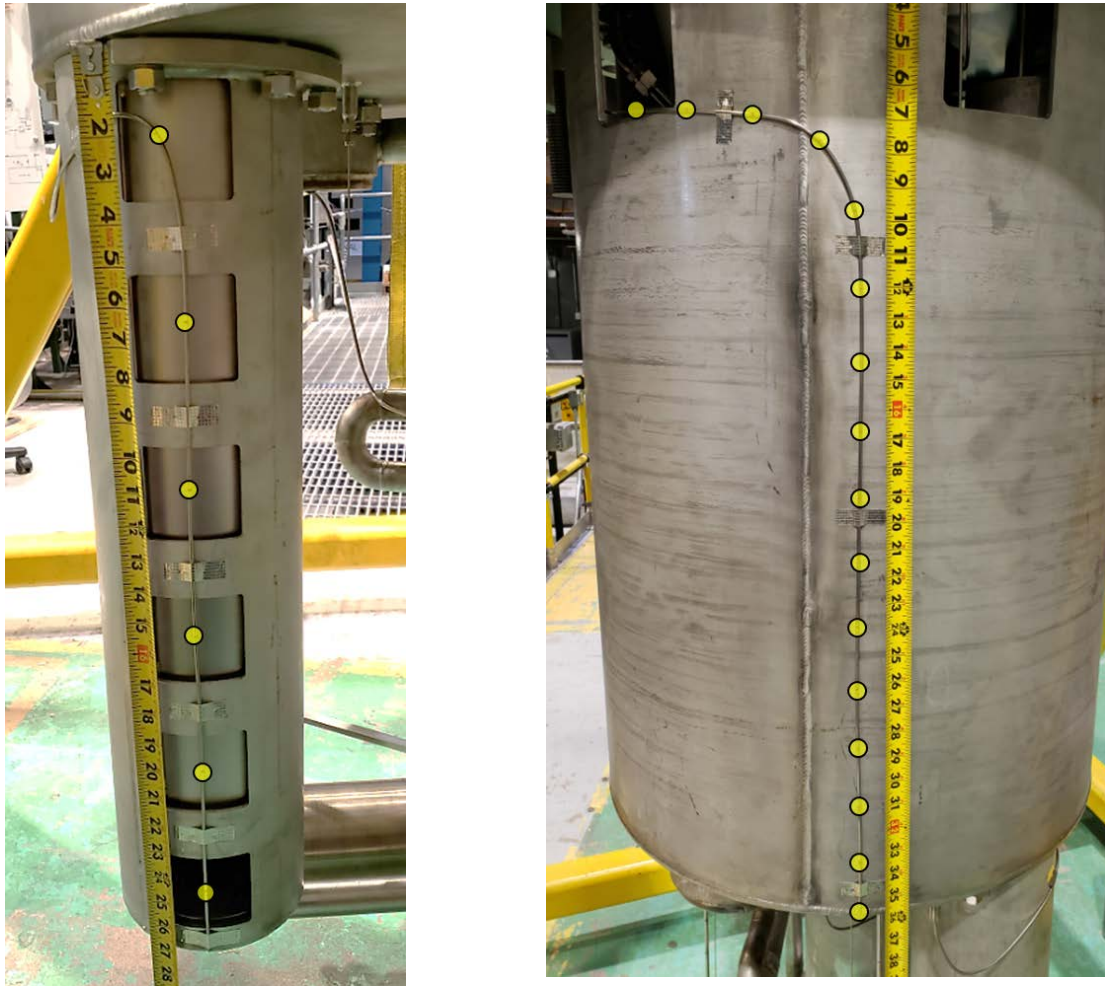


Figure 30: LEFT: intermediate heat exchanger outlet showing 1/8" multijunction thermocouple probe with junctions at the center of each of the 6 outlets. 0.008" thick 316 stainless steel sheet metal was used to fix the position of the probe. QTY (6) thermocouple junction locations were highlighted with yellow circles for clarity. RIGHT: Temperature is read on the outer surface of the inner vessel with the use of a 1/8" multijunction thermocouple probe. QTY (16) thermocouple junction locations were highlighted with yellow circles for clarity.

The THETA submersible electromagnetic flowmeter was mounted in primary loop circuit, the signal and thermocouple feed through wires were fed out of the sodium and vapor space through ports 12a and 12b, respectively, Figure 31.

A custom-built single point electrical continuity level detector was installed in port 11 to allow for precise level determination, Figure 32. The level sensor is set to signal full when the hot pool level is at an elevation of 23" above the bottom of the inside of the inner vessel.

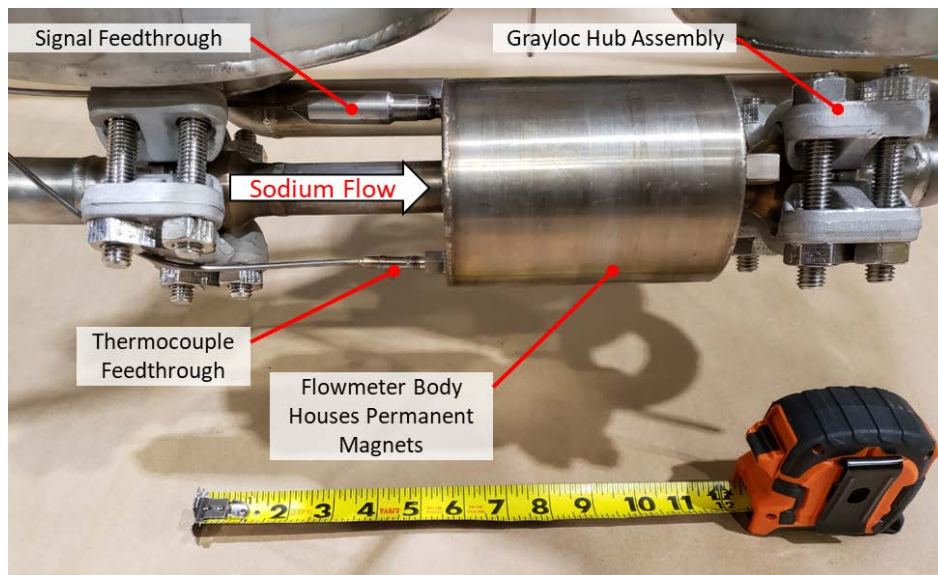


Figure 31: Electromagnetic flowmeter installed in THETA primary piping. All 316 stainless steel Grayloc assemblies with Inconel uncoated seal rings are used.



Figure 32: Custom built single point continuity level detector. All stainless steel and alumina construction. BNC connector for sensor reading.

3.4. Submersible Flowmeter

A submersible permanent magnet flowmeter has been designed to acquire primary sodium flowrate, Figure 31. The flowmeter uses a magnetic field generated by high temperature Samarium-Cobalt (SmCo) magnets, oriented perpendicular to sodium flow, to generate a Lorentz current that is linearly proportional to flow. A complete description of the design and construction of the flowmeter can be found in [1], [2]. A peer-reviewed journal publication in IEEE Sensors details the complete design, calibration, and uncertainty propagation of the flowmeter [4].

The submersible flowmeter sensor wires were exposed during calibration in an auxiliary sodium loop to allow for modification if necessary, Figure 33. The flowmeter was then brought to a vendor where the flowmeter was hermetically sealed with the use of precise TIG welding under a microscope. As can be seen in Figure 34, the signal wires were welded to the MI cable feedthrough. A small rectangular piece of 0.030" thick alumina electrical insulator (insulator #2 in Figure 34) was then installed to separate the signal wires. A tube shaped electrical insulator was then slid over the sensor wires (insulator #1), followed by the signal wire shroud. The shroud was then micro welded to the flowmeter body and the MI cable feedthrough to provide a completely hermetic seal.

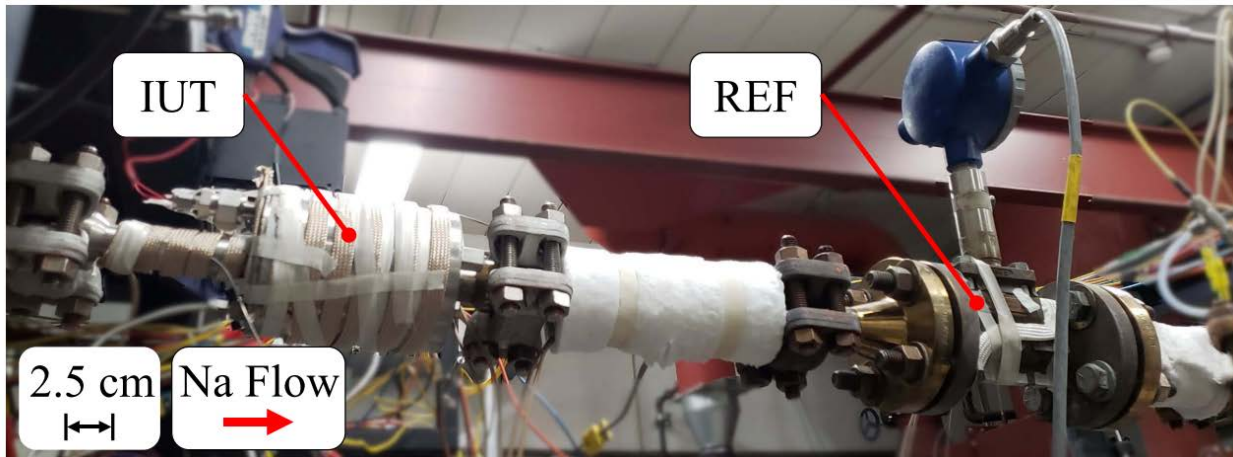


Figure 33: Photo showing the Instrument Under Test (IUT) and the Reference (REF) flowmeter installed in the University of Wisconsin-Madison liquid sodium calibration loop. The loop possesses a moving magnet pump that is controlled by a variable frequency drive

In order to pull vacuum and backfill with a cover gas, a backfill port is present on the thermocouple feedthrough, Figure 35. A vacuum was pulled with the turbo pump on the helium leak detector to evacuate any contaminant gasses in the flowmeter to a pressure of <1 milliTorr. A wand was then used to pass helium across all surfaces of the flowmeter. A helium leak rate of 10^{-8} atm-cc/sec was achieved during this operation, a satisfactory result, Figure 36 and Figure 37. The flowmeter cavity was then backfilled to a helium pressure of 23 inH₂O (0.83 PSIG). This will yield an internal helium cavity pressure of 13 PSIG at 250 °C and 26 PSIG at 500 °C. The vacuum/helium backfill port was then crimped shut and immediately TIG welded to hermetically seal the cavity Figure 35. A photo of the complete flowmeter ready for installation can be seen in Figure 38.

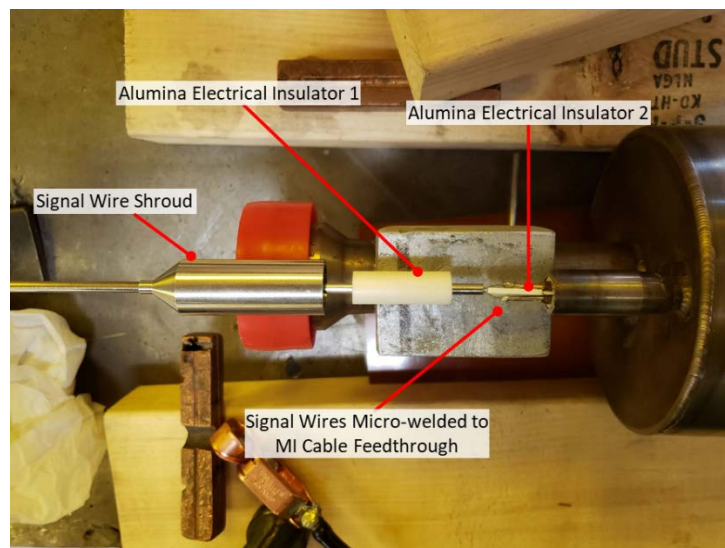


Figure 34: Sealing off signal wire feedthrough on THETA primary flowmeter.

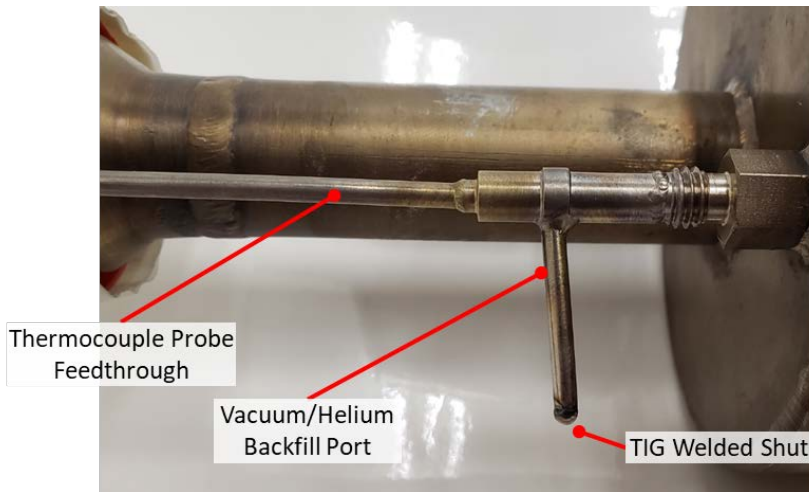


Figure 35: Vacuum/helium backfill port TIG welded shut

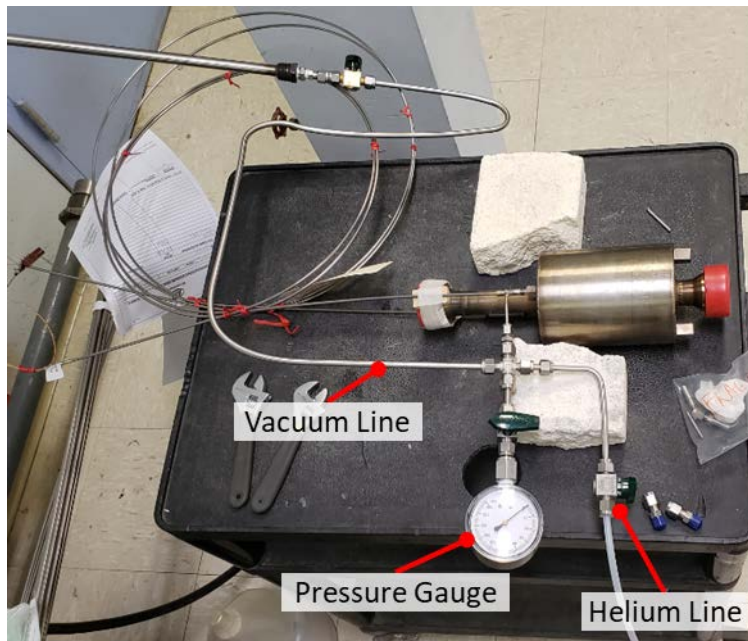


Figure 36: Setup to facilitate pulling vacuum and backfilling flowmeter cavity with helium.

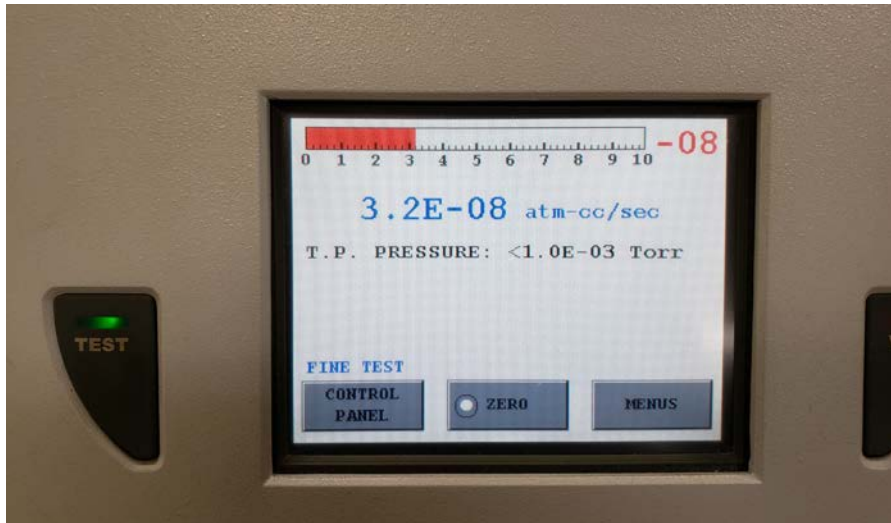


Figure 37: Helium leak detector showing hard vacuum of <1 milliTorr pulled on assembly and a helium presence of 10^{-8} atm-cc/sec in the internal cavity of the flowmeter where signal wires, thermocouple and magnets reside. Helium gas was passed across all surfaces of the flowmeter.



Figure 38: Photo of completed THETA submersible electromagnetic flowmeter with 15" ruler for reference. Note the 1/8" MI cables transmitting temperature and sensor data have been spooled up for easy transport

A magneto-hydrodynamic CFD model was developed to model the flowmeter using COMSOL-Multiphysics software. Figure 39 provides a representation of the CFD model depicting the velocity of sodium flowing through the 1" flow tube as well as the magnetic flux density in the vicinity of the permanent magnets [4]. Note that as the sodium passes across the magnetic flux of

the magnets there is a ‘smoothing’ effect on the velocity profile due to Lorentz force and the profile becomes more homogenous across the tube cross section.

Experimental data taken while calibrating the flowmeter can be found in Figure 40 [4]. Notice the finite element analysis results from the CFD model are also included and show very good similitude with experimental results. Error bars for the experimental results were calculated using propagation of error in [4]. An uncertainty budget in Table 2 provides the uncertainties of the constituent experimental variables used to calculate sodium flowrate.

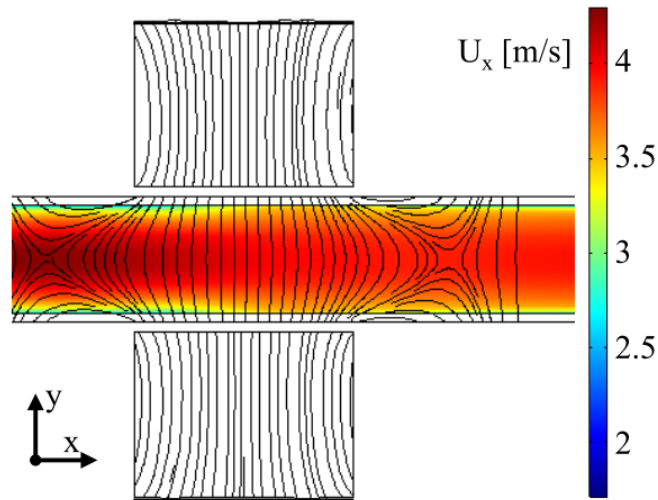


Figure 39: Velocity in the x direction, U_x , with black streamlines showing magnetic flux density through the cross section of the flow tube and permanent magnets. T_m and T_s at 400 °C, $Q= 83.3$ LPM (22 GPM) [4]

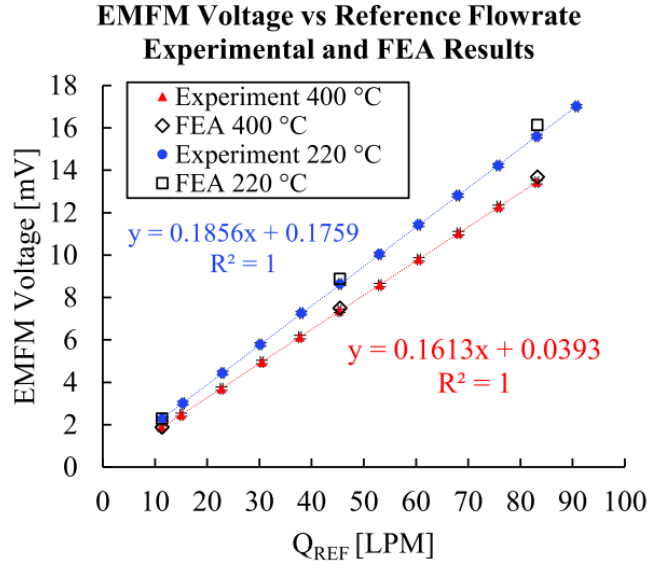


Figure 40: Experimental and FEA induced voltage as a function of sodium flowrate at 400 and 220°C. FEA results deviate <3.2% from experimental trendline. Error bars have been provided for EMFM voltage and reference flow rate, representing type A and B uncertainty in the 90 measurements taken for each flow rate and temperature [4]

Table 2: Electromagnetic Flowmeter Uncertainty Budget [4]

Variable	Source	$U_{C,\sigma}, U_{s,i}$	$U_{b,i}$
C	$U_{C,\sigma}$	6.02E-04	-
T_m, T_s	Thermocouple	-	± 3.0 °C
	NI 9213	-	± 1 °C
Q_{REF}	Calibr. Cert.	$\pm 0.5\%$	-
	NI 9219	$\pm 0.3\%$	± 4.5 mV
B	Gaussmeter	-	± 0.1 mT
V_m	NI 9219	$\pm 0.1\%$	± 0.08 mV
	Lead Position	-	$\pm 0.2\%$
L, d, D	Calipers	-	± 0.025 mm

Flowmeter at $\approx 400^\circ\text{C}$, 22.7 LPM (6 GPM). The thermocouples are Omega type K, ungrounded 3.2 diameter probes. NI 9213 and 9219 are National Instruments data acquisition modules connected to a National Instruments cRIO 9024 chassis. The Gaussmeter is an F.W. Bell model 5180. The calipers are Mitutoyo model 500-474.

3.5. Installation of Primary Assembly

Following final sanitization and assembly of the primary assembly, THETA was transported to METL 28” vessel #4 with the use of the 5-ton overhead crane in the Building 308 hibay, Figure 41 and Figure 42. THETA as installed in the vessel can be seen in Figure 3. After installing THETA, the flange heaters and insulation were then installed, Figure 43. All of the 120+ thermocouples, flowmeter signal wires, level sensor, etc. were connected. Finally, all of the electrical control and data acquisition cabinets for THETA were installed on the North side of the METL mezzanine, Figure 44.



Figure 41: Installation of THETA into METL with building 308 overhead crane

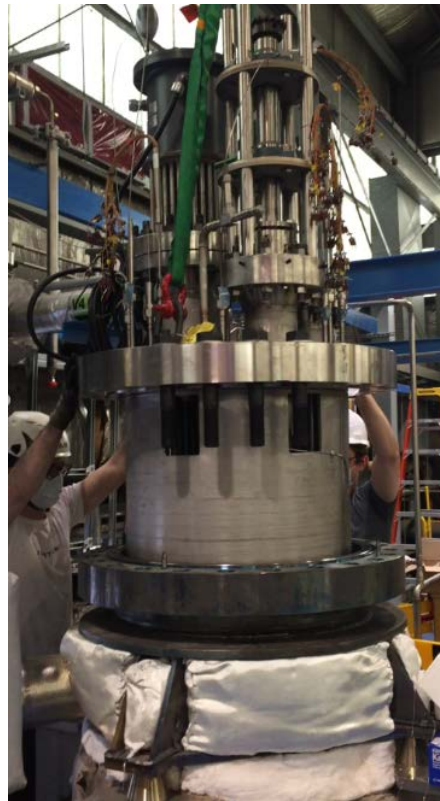


Figure 42: Installation of THETA into METL with building 308 overhead crane



Figure 43: THETA with flange heaters, insulation, pump motor, and all thermocouples and instrumentation installed

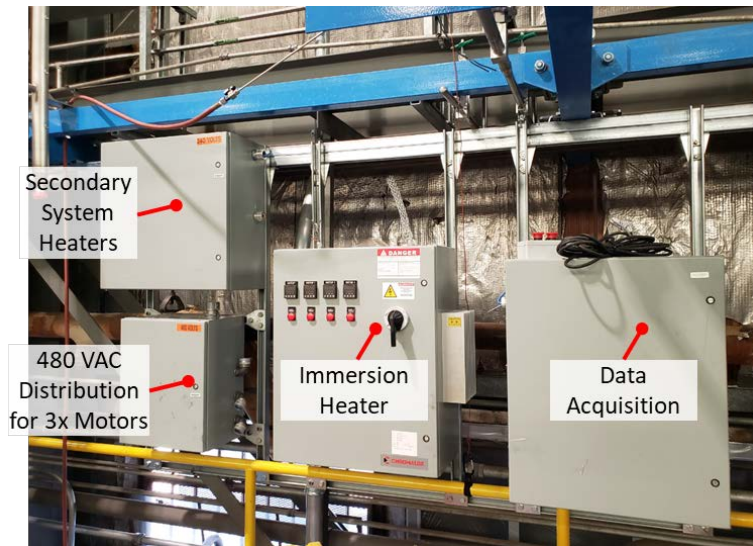


Figure 44: THETA electrical control cabinets installed on METL mezzanine, north wall

3.6.Data Acquisition and Control Software

Software that facilitates the data acquisition of the various sensors (thermocouples, flowmeters, level sensor etc.) as well as the control of THETA components (pump, immersion heater etc.) was developed. Labview 2018 was used to develop the program- a screenshot of the user interface can be found in Figure 45. As can be seen on the left side of the program, all of the thermocouple rake temperatures are shown in real time, where the thermocouple junctions in the hot pool possess a red colored backdrop while junctions in the cold pool possess a blue colored backdrop for quick dissemination of location.

The immersion heater control panel is located in the top center of the graphical user interface (GUI). This panel allows the user to monitor the process control thermocouple, set the gain values for PID control, monitor the status of the solid state relay, provide a maximum wattage output limit as well as set a trigger for when to activate or deactivate the heater at a specific time to facilitate reactor trip simulations.

The pump control panel is located in the top right of the GUI. As can be seen- the operator is able to monitor pump shaft vibration and flowrate as well as set pump speed and maximum speed and vibration limits. Under the pump control panel the user will find a pair of variable plotters, allowing the user to select and plot any system parameter in real time.



Figure 45: Labview based graphical user interface, THETA data acquisition and control software

3.7. METL 28” Flange Fastener Improvement

Significant galling was seen in previous testing when pairing 304 stainless steel nuts with 304 stainless steel bolts to mount a blank 28” flange to the METL vessel at a temperature of ~500 °C, even with the use of nuclear grade nickel based high temperature anti-seize, Figure 46. Galling was seen in approximately 4 of the 24 fasteners. 3 of the galled bolts were removed with the use of a high torque hydraulic wrench, the remaining galled bolt was removed with a reciprocating saw. 1-1/2”-12 heavy hex nuts in Inconel 718, SB-637 with silver coating were acquired to mate with 304 stainless steel bolts to seal the THETA flange to the 28” METL vessel flange, Figure 47. The use of dissimilar metals and the interstitial silver plating should provide superior galling resistance.



Figure 46: 1-1/2” 304SS flange bolt with galling

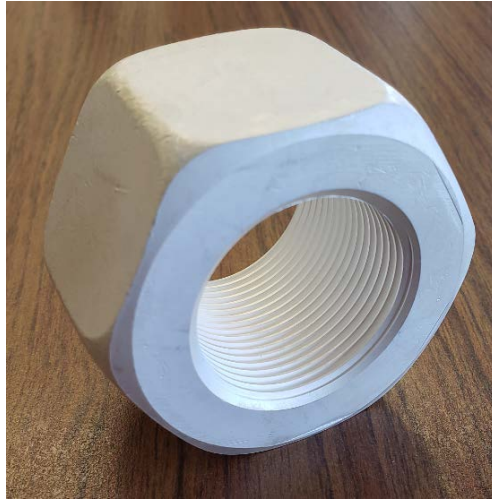


Figure 47: Significant galling was seen when pairing 304 stainless steel nuts with 304 stainless steel bolts to mount the THETA flange to the METL vessel, even with the use of nuclear grade high temperature anti-seize. 1-1/2”-12 heavy hex nuts in Inconel 718, SB-637 with silver coating were acquired to mate with the stainless steel flange bolts

4. Secondary System

4.1. Secondary Flowmeter

A permanent magnet flowmeter was designed to acquire sodium flow rate in the THETA secondary loop, Figure 48. The sodium flows through a 3/4” SCH 40 stainless steel pipe where a magnetic field interacts with the flowing sodium to produce a voltage signal. A thermal analysis study was performed on the flowmeter where the flow pipe was set to a temperature of 670 °C and the surface temperature of the flowmeter components were characterized Figure 49. It is important that the magnet temperature stay near room temperature, especially for powerful Neodymium magnets which possess a maximum operating temperature of ~80°C. A preliminary magnetohydrodynamic finite element analysis was run to assess the induced voltage of the flowmeter at a nominal 5 GPM flowrate, Figure 50. A signal of 3.4 mV is predicted at 5 GPM.

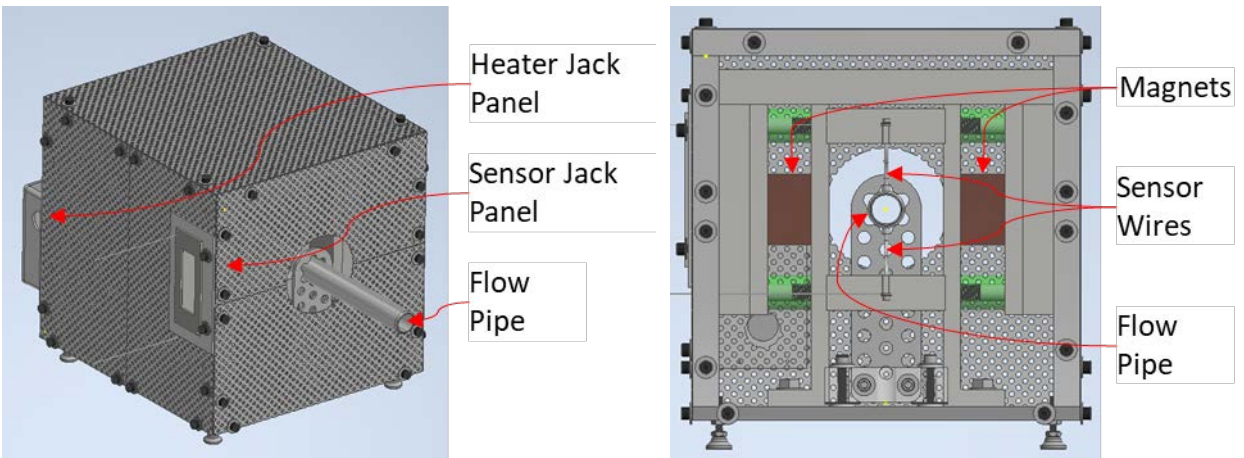


Figure 48: Secondary flowmeter isometric view (left), view with grating removed to reveal important constituent components (right)

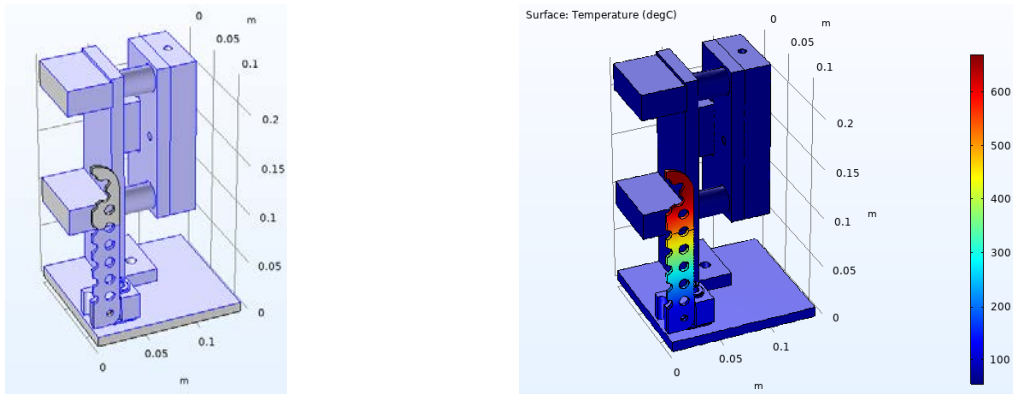


Figure 49: Secondary flowmeter surfaces with convection coefficient set to $1 \text{ W/m}^2\text{K}$ shown in blue, all other surfaces adiabatic (left). Surface temperature profile with flow pipe temperature set to $670 \text{ }^\circ\text{C}$ (right).

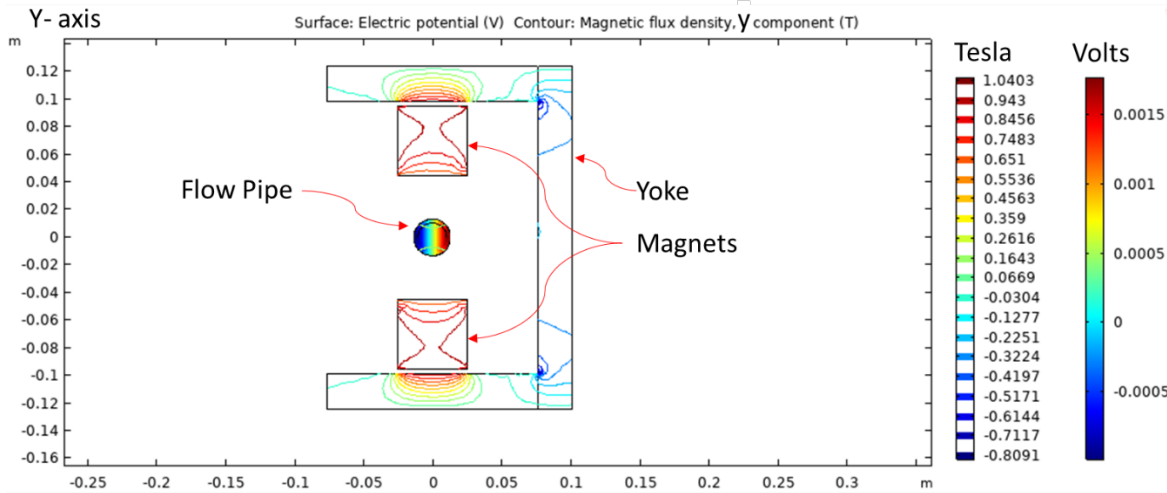


Figure 50: COMSOL Multiphysics study, cross section looking down flow pipe at the center of the magnet/yoke assembly showing the electric potential and magnetic flux density at a sodium flowrate of 5 GPM

4.2. Secondary Pump

A pump was ordered for the THETA secondary loop. The pump is of the AC conduction variety from CMI-Novacast, part number CA-15. A photo of a CA-15 pump and the pump curves can be found in Figure 51.

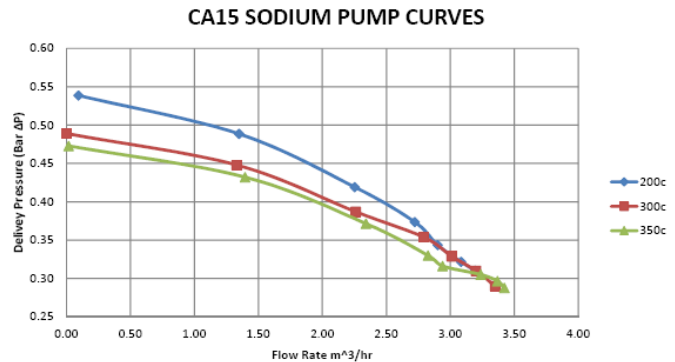


Figure 51: THETA secondary pump and pump curves

4.3. Intermediate Heat Exchanger

A design for the intermediate heat exchanger (IHX) has been finalized and machine drawings produced, Figure 52. The IHX possesses a vacuum insulated downcomer to better represent the counter flow heat exchange in a typical SFR, where a large downcomer transports sodium to the bottom of the exchanger in the hot pool, limiting the amount of heat exchange. Then, the sodium flows up through a large number of upcomer tubes where the surface area, and thus the heat

exchange, is enhanced, Figure 53. In order to reduce the heat exchange in the downcomer tube, it is double walled, whereby a vacuum is able to be pulled in the annular region between the walls with a snorkel that extends from the top of the downcomer to the top of the heat exchanger flange, snorkel shown in green in Figure 54. Given the walls of the downcomer and upcomers will be at different temperatures, given the differential in heat exchange, a pair of thermal expansion bellows will serve to relieve thermal stress, Figure 53 and Figure 54.

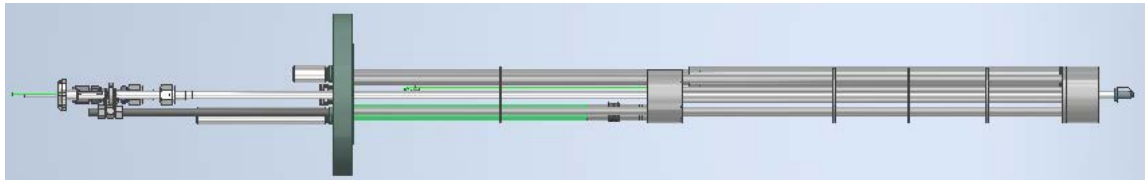


Figure 52: THETA IHX side view

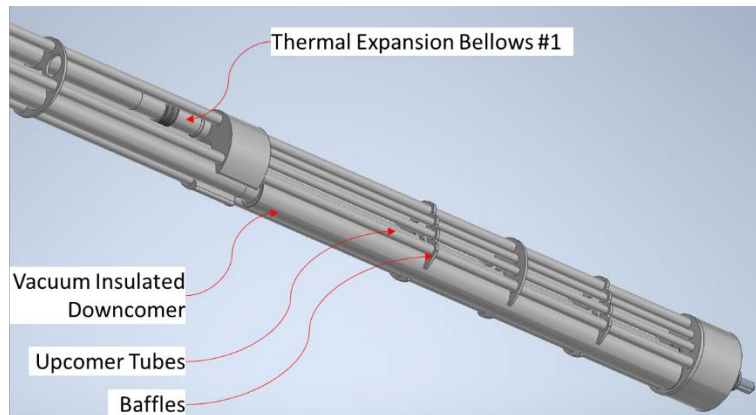


Figure 53: IHX view showing the downcomer/upcomers and baffles

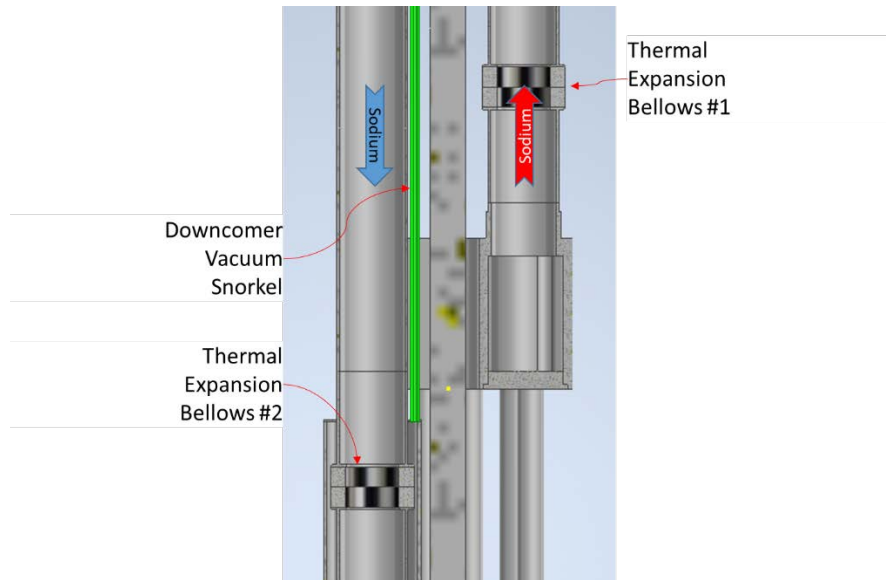


Figure 54: Cross section showing the two thermal expansion bellows and the downcomer vacuum snorkel

5. THETA Model Development

Modeling of the Thermal Hydraulic Experimental Test Article (THETA) experiment has been performed using the SAS4A/SASSYS-1 fast reactor safety analysis code. A THETA model has been developed to represent the THETA experiment design developed at Argonne to demonstrate the importance of key elevations on natural circulation flow rates. The model currently includes the core channel and the primary heat transport system of the THETA experimental facility. A summary of this work can be found in [2].

6. Conclusions and Path Forward

THETA has completed the commissioning phase of its development for insertion into METL. All major components of the primary system have been installed in METL vessel #4. All data acquisition and control systems are operational and the data acquisition and control software is functioning. The vessel was brought to a temperature of 100 °C and the pump was jogged to ensure proper functionality. The next step will be to fill vessel #4 with sodium at a temperature of 200 °C and commence shakedown testing in sodium. THETA will then be ready to pursue an experimental campaign.

7. Acknowledgements

The authors would like to acknowledge Daniel Andujar of the METL team for all his hard work and dedication to supporting the commissioning of the THETA test article. The authors would also like to acknowledge Dzmity Harbaruk and Henry Belch for their assistance. This work is funded by the U.S. Department of Energy Office of Nuclear Energy's Advanced Reactor Technologies program. A special acknowledgement goes to Mr. Brian Robinson, Fast Reactor Program Manager for the DOE-NE ART program and to Dr. Robert Hill, the National Technical Director for Fast Reactors for the DOE-NE ART program for their consistent support of the Mechanisms

Engineering Test Facility and its associated experiments, including the Thermal Hydraulic Experimental Test Article (THETA). Prior years' support has also been provided by Mr. Thomas O'Connor and Mr. Thomas Sowinski of U.S. DOE's Office of Nuclear Energy.

8. References

- [1] Weathered *et al.*, “Thermal Hydraulic Experimental Test Article – Status Report FY2020,” Lemont, 2020.
- [2] M. Weathered *et al.*, “Thermal Hydraulic Experimental Test Article – Status Report for FY2019 Rev. 1,” Lemont, 2019.
- [3] T. Sumner and A. Moisseytsev, “Simulations of the EBR-II Tests SHRT-17 and SHRT-45R,” in *16th International Topical Meeting on Nuclear Reactor Thermal Hydraulics (NURETH-16)*, 2015.
- [4] M. Weathered, C. Grandy, M. Anderson, and D. Lisowski, “High Temperature Sodium Submersible Flowmeter Design and Analysis,” *IEEE Sens. J.*, vol. 21, no. 15, pp. 16529–16537, 2021.



Nuclear Science and Engineering

Argonne National Laboratory
9700 South Cass Avenue, Bldg. 208
Argonne, IL 60439

www.anl.gov



Argonne National Laboratory is a U.S. Department of Energy
laboratory managed by UChicago Argonne, LLC